Development 135, 183-192 (2008) doi:10.1242/dev.010363

Regulated addition of new myocardial and epicardial cells fosters homeostatic cardiac growth and maintenance in adult zebrafish

Airon A. Wills, Jennifer E. Holdway, Robert J. Major and Kenneth D. Poss*

The heart maintains structural and functional integrity during years of continual contraction, but the extent to which new cell creation participates in cardiac homeostasis is unclear. Here, we assessed cellular and molecular mechanisms of cardiac homeostasis in zebrafish, which display indeterminate growth and possess an unusual capacity to regenerate after acute cardiac injury. Lowering fish density in the aquarium triggered rapid animal growth and robust cardiomyocyte proliferation throughout the adult ventricle, greater than that observed during slow animal growth or size maintenance. Rapid animal growth also induced strong expression of the embryonic epicardial markers *raldh2* (*aldh1a2*) and *tbx18* in adult epicardial tissue. Pulse-chase dye labeling experiments revealed that the epicardium recurrently contributes cells to the ventricular wall, indicating an active homeostatic process. Inhibition of signaling by Fibroblast growth factors (Fgfs) decreased this epicardial supplementation of the ventricular wall in growing zebrafish, and led to spontaneous ventricular scarring in animals maintaining cardiac size. Our results demonstrate that the adult zebrafish ventricle grows and is maintained by cardiomyocyte hyperplasia, and that epicardial cells are added to the ventricle in an Fgf-dependent fashion to support homeostasis.

KEY WORDS: Cardiomyocyte, Epicardium, Heart, Regeneration, Tissue homeostasis, Zebrafish

INTRODUCTION

Organ homeostasis mechanisms calibrate organ size and function in response to changing physiological conditions. Perhaps the clearest example of homeostasis occurs during animal growth, a process accompanied by organ growth to accommodate increasing demands. For full-sized adult mammals, homeostasis maintains the status quo, replacing damaged or senescent cells through direct structural cell proliferation, progenitor cell activity or hypertrophy of surrounding cells. Some organs are capable of rapid homeostatic adjustments to tissue loss or gain. For example, the liver will increase mass through compensatory cell proliferation after partial hepatectomy, or reduce mass through compensatory cell death after experimentally induced hyperplasia, to maintain the appropriate size (Conlon and Raff, 1999; Potter and Xu, 2001; Taub, 2004). Understanding the cellular and molecular mechanisms of organ homeostasis is a major research goal, with potential to shed light on therapies for trauma, degenerative disease and aging.

Although cellular and molecular mechanisms of homeostatic regulation in most organs are incompletely understood, cardiac homeostasis is particularly mysterious. For many years, it was believed that the adult mammalian heart is a post-mitotic organ, and that all postnatal cardiac growth is achieved through hypertrophy of a fixed number of cardiomyocytes (CMs). Indeed, analyses of DNA synthesis in the adult murine heart estimated a very low percentage (a maximum of 0.0005%) of ventricular CMs entering the cell cycle each day (Soonpaa and Field, 1997). Similar analyses during postnatal rodent growth indicated that CMs undergo a transition shortly after birth from hyperplastic to hypertrophic growth, associated with the production of large, multinucleated CMs through karyokinesis rather than with new, mononucleated CMs through cytokinesis (Li et al., 1996; Soonpaa et al., 1996). Furthermore, there is little evidence of consequential regeneration after cardiac injuries such as ischemic infarction, and the resulting hypertrophy of existing muscle that occurs concomitantly with scar formation is detrimental to cardiac function. The notion that the major structural cells within such a vigorous and vital organ survive 70 to 100 years in humans without support from new CMs is contested, especially given recent identification of cell populations that may possess progenitor activity in the postnatal mammalian heart (Beltrami et al., 2003; Laugwitz et al., 2005; Martin et al., 2004; Oh et al., 2003). However, a natural in vivo contribution of these progenitor cells to adult tissue homeostasis has not been experimentally demonstrated.

The mechanisms by which non-myocardial cardiac cell types are maintained and replaced are also poorly understood. Interestingly, recent studies have found that cells of the adult mammalian epicardium, a thin epithelial tissue surrounding the myocardium proper, can be experimentally stimulated to differentiate into smooth muscle and endothelial cells in vitro (Smart et al., 2007; van Tuyn et al., 2007). In this way, the in vitro activity of the adult epicardium appears to mimic the capacity of the embryonic epicardium, a structure that serves as the primary source of coronary vasculature during heart development (Reese et al., 2002). Thus, it is possible that adult epicardial cells also function as a progenitor tissue to maintain the vasculature or other cardiac cell populations.

Certain non-mammalian vertebrates such as amphibians and fish may have greater potential for hyperplastic cardiac homeostasis. By contrast with mammals, many of these species display indeterminate growth, and can rapidly increase adult mass in response to changes in population density and nutrition (Jordan, 1905), an increase that is typically accompanied by organ augmentation. Moreover, some of these species have demonstrated various degrees of regeneration after mechanical injury of the cardiac ventricle, a response that may be perceived as a homeostatic method to restore cardiac mass (Flink, 2002; Oberpriller and Oberpriller, 1974; Poss et al., 2002). In

Department of Cell Biology, Duke University Medical Center, Durham, NC 27710, USA.

*Author for correspondence (e-mail: k.poss@cellbio.duke.edu)

Accepted 1 October 2007

particular, the zebrafish, which displays indeterminate growth (Tsai et al., 2007), has a strong cardiac regenerative response, and is amenable to molecular genetic approaches, represents a unique model system to visualize and dissect cardiac homeostasis.

Here, we show that adult zebrafish display dramatic, hyperplastic cardiac growth in response to aquarium conditions that stimulate rapid animal growth, whereas animals maintaining cardiac size show distinct but rare addition of new CMs. Additionally, we find that rapid growth conditions induce epicardial expression of embryonic markers such as *raldh2* (also known as *aldh1a2* – Zfin) and *tbx18*, and that the epicardium regularly contributes cells to the adult ventricular wall even in the absence of cardiac growth or myocardial injury. Inhibition of Fgf signaling, a pathway necessary for normal heart regeneration, disrupts epicardial cell supplementation and causes spontaneous ventricular scarring in uninjured adult fish. Our study exposes dynamic myocardial and epicardial mechanisms that mediate cardiac homeostasis.

MATERIALS AND METHODS

Zebrafish

Zebrafish of outbred Ekkwill or EK/*AB mixed background strains were raised at a standard density of approx. five fish per liter to 8-10 weeks of age, at which point fish weighing 70-100 mg were selected for growth experiments. Fish were placed in conditions that stimulate rapid growth (RG; 3 fish/10 l tank) or returned to conditions that allow normal, slower growth (SG; 15 fish/3 l tank) for 10-14 days, at which point the animals were weighed and the hearts extracted. Adult fish, 6-months old, maintaining animal size (MS) were raised at 3-5 fish/l, the standard in our facility. Ventricular resection surgeries were performed as previously described (Poss et al., 2002). All experiments on animals were performed in accordance with institutional guidelines and regulations.

Histological techniques

In situ hybridization on cryosections of paraformaldehyde (PFA)-fixed hearts was performed using digoxigenin-labeled cRNA probes as described previously (Poss et al., 2002). Acid fuchsin-Orange G staining was performed as described previously (Poss et al., 2002). Immunofluorescence was performed (Poss et al., 2002) using antibodies against BrdU (rat; Accurate), Mef2 (rabbit; Santa Cruz Biotechnology), PCNA (mouse; Sigma) and DsRed (rabbit; Clontech). Terminal deoxynucleotidyl transferase biotin-dUTP nick end-labeling (TUNEL) reactions were performed on 10 μm cryosections of PFA-fixed hearts with reagents from Invitrogen, and visualized with peroxidase substrate reagents from Vector Laboratories.

Ventricular size, CM BrdU incorporation, CM density, %RFP^{cyto} cells and EPDC density

To calculate ventricular section surface area, hearts were sectioned longitudinally, stained with TRITC-phalloidin, and the three largest sections of the ventricle were imaged and measured for calculation of the area using Openlab software. The measurements were averaged to give one value for each heart.

For BrdU incorporation experiments, animals were injected once daily with 2.5 mg/ml BrdU for 3 days prior to collection. Hearts from RG (injected 7, 8 and 9 days after introducing density conditions), SG, and MS animals were cryosectioned and immunostained for Mef2 and BrdU. Images of the middle of the lateral ventricle wall (opposite the atrium) from the three largest sections of each ventricle were selected for analysis. Nuclei labeled with Mef2, a marker of CMs, BrdU, or both were counted by hand using Adobe Photoshop images. The region analyzed included the compact muscular wall and a region approximately six cells thick of trabecular muscle, so that both trabecular and compact muscle would be included. For these experiments, 150-300 Mef2^{pos} nuclei were counted per section, or 500-900 per animal.

To calculate CM density, Mef2-stained ventricular sections were used to produce similar images. Then, the area of the region was calculated using Openlab software, and the number of CM nuclei within the traced region counted by hand. About 100-300 nuclei were counted per section, or 400-900 per animal. To assess CM nucleation, ventricles were isolated from *cmlc2:nRFP* RG, SG and MS fish (see Results for description of transgenic zebrafish), and cells were dissociated as described previously (Warren et al., 2001). Isolated cells were collected in L-15 medium and live cells imaged to determine the number of nuclei.

For analysis of RFP^{cyto} cells (see Results for RFP^{cyto} description), cryosections from *cmlc2:nRFP* ventricles were stained with anti-DsRed antibody and the three largest sections from each heart were used for imaging. For these experiments, images of the apex were selected for analysis. RFP^{nuc} and RFP^{cyto} cells were counted by hand from regions including the ventricular wall and approximately four cell layers of trabecular muscle. About 150-300 CMs per section were counted, or 600-900 per animal.

For analysis of epicardial-derived cells (EPDCs) within the ventricular wall, in situ hybridizations for *tbx18* were performed on hearts from wild-type or *hsp70:dn-fgfr1* animals under various growth conditions. Images from the middle of the lateral ventricle wall (opposite the atrium) were taken from the three largest sections of each heart. For each section, only *tbx18*-positive cells clearly separated from the epicardium and within the compact myocardial wall were counted (see Figs 5 and 6).

RNA isolation and real-time Q-PCR analysis

RNA was collected from 12-15 MS, RG, SG and regenerating [7 days post-amputation (dpa)] ventricles by extracting the heart in PBS on ice and mechanically removing the atrium and outflow tracts. Ventricles were transferred to TRI reagent (Sigma) and the RNA was isolated according to the manufacturer's instructions, before purification using Qiagen RNAeasy columns. RNA integrity was assessed by gel electrophoresis, and concentration determined by spectroscopy. cDNA was made from 200 ng RNA using oligo(dT) primer and SuperScript III reverse transcriptase (Invitrogen). Quantitative PCR (Q-PCR) was run using LightCycler FastStart DNA Master^{PLUS} SYBR Green I (Roche) on a LightCycler 2.0 machine (software version 4.05x). Dilutions of cDNA generated from pooled RNA of 20 hours and 56 hours post-fertilization embryos was used to determine the reaction efficiency (E) for each primer pair, and ΔC_T for each group was calculated using 7 dpa regenerating hearts as a standard. *hand2* expression was normalized to *gapdh* for each sample using the following equation: $X=((E_{gapdh})^{-\Delta CT gapdh}) / ((E_{hand2})^{-\Delta CT hand2})$. All samples were run in triplicate, and the averages of two independent experiments are shown.

Pericardial manipulations

Adult zebrafish ~6 months of age were placed into 1.5 l tanks (3 fish/l) to maintain a constant density during the experiment. Hearts from uninjured control animals, as well as manipulated animals, were fixed 3 days after manipulations. In one group of animals (Open), a single incision was made in the pericardial sac using iridectomy scissors. In saline-treated animals, ~5 μl Hank's buffered saline was injected into the pericardial cavity from a 30 gauge needle until expansion of the sac was visible. For an additional group, a needle was similarly inserted into the pericardial sac, but no fluid was injected (Pierce). Only animals that showed no bleeding after any of these treatments were used for this study. As a control, iridectomy scissors were used to make a small incision on the dorsal side of the animal (Dorsal). For each group 9-11 animals were used in two experimental trials.

DiI labeling of the adult epicardium

DiI labeling was performed by pipetting ~0.5 μl of 1 mg/ml Cell Tracker CM-DiI (Molecular Probes) into the pericardial cavity of ~6-month-old zebrafish through a small incision in the pericardial sac. Smaller animals used for RG and SG conditions did not survive this procedure. Hearts were extracted and fixed at 1 hour, 3 days, 7 days and 14 days post-labeling. Labeled hearts were sectioned and imaged without coverslips, as mounting with a coverslip commonly caused diffusion of the dye. At least 15 animals were used for 1 hour, 3 day, and 7 day timepoints in three experimental trials.

Fgfr inhibition

For RG experiments, heterozygous *hsp70:dn-fgfr1* transgenic and wild-type clutchmates (weighing 70-100 mg each) were selected at 8-10 weeks of age. Fish received a daily, transient increase in temperature from 26°C to 38°C as described previously (Lee et al., 2005). Animals remained at 38°C for ~30

minutes each day. We found that this temperature increase could not be achieved in 10 l tanks using our system, so we instead placed one fish each in a 3 l tank, and performed analyses at 14 days. For adult maintenance experiments, uninjured 4- to 6-month-old *hsp70:dn-fgfr1* and wild-type adult clutchmates received a daily temperature increase for 60-70 days.

RESULTS

Experimental control of adult cardiac homeostasis

We predicted that the vigor of cardiac homeostasis would be proportional to the rate of adult animal growth. Therefore, we developed three conditions based on aquarium density that we expected to stimulate rapid growth (RG), slow growth (SG) or size maintenance (MS). We found that when small adult fish (8- to 10-weeks old, 70-100 mg) were removed from standard aquarium density conditions (SG; 5 fish/l) and placed in low-density conditions (RG; 0.3 fish/l), body mass tripled after only 14 days (a ~208% increase from day 0). Clutchmates maintained at SG displayed only a ~13% increase in mass over this period. Fully mature, 6-month-old fish, considerably larger at the onset of experiments than RG and SG fish, maintained mass for at least 28 days when kept at standard aquarium density conditions (Fig. 1B). In general we found that starting size was a greater determinant of animal growth rate than age, consistent with other published studies (Tsai et al., 2007).

In these experiments, the large increases in body mass seen in RG fish were accompanied by dramatic increases in the size of both heart chambers (Fig. 1A). To quantify changes in ventricular size, we measured the surface area of longitudinal ventricular sections using digital imaging software. These analyses revealed that ventricular size more than tripled after only 14 days in RG conditions (a ~221% increase from day 0), a rate of cardiac growth approximately equivalent to that of animal growth under these conditions. Clutchmates in SG conditions exhibited a more modest increase in ventricular size over this period (~48%). Because this increase was greater than the increase in animal size during this period, it is possible that the rate of cardiac growth may slightly diverge from the rate of animal growth in SG conditions. MS animals experienced no significant change in ventricular size over 14 days (Fig. 1A,C). Thus, by varying aquarium density and starting size of the animal, we closely controlled the rate of cardiac homeostasis. In particular, low aquarium density conditions induced remarkably rapid cardiogenesis in adult zebrafish.

New cardiomyocyte creation accompanies cardiac growth and maintenance

To determine whether density-dependent control of ventricular size resulted from hyperplasia or hypertrophy, we administered three daily injections of BrdU prior to harvesting tissue after 9 days in RG, SG or MS conditions. CMs were specifically assayed for BrdU incorporation by costaining with an antibody against Mef2, a transcription factor that regulates myocardial differentiation (Molkentin and Markham, 1993). We observed a high rate of BrdU incorporation in CMs within both trabecular and compact muscle compartments of RG fish, with 10.1±1.8% of CMs labeled by BrdU (mean ± s.e.m.; Fig. 2A,B). This labeling index was almost eight times that of SG animals (1.3±0.3%), and 25 times that of MS animals sustaining constant body mass and ventricular size (0.4±0.1%; Fig. 2A,B). We obtained similar results when identifying proliferating cells with an antibody against PCNA (see Fig. S1 in the supplementary material). We suspect that rare CM proliferation in MS animals serves to replace dying cells, as we observed occasional CM apoptosis events by TUNEL staining of ventricular sections (see Fig. S2 in the supplementary material).

To assess possible contributions of hypertrophy to growth, we measured the density of cells positive for the nuclear marker Mef2 in ventricular sections. There were no differences in CM nuclear density per myocardial area in RG, SG and MS fish, indicating a lack of CM hypertrophy (Fig. 2C). In addition, we dissociated ventricles and assessed the extent of binucleation, a consequence of karyokinesis without cytokinesis that is common in adult mammalian CMs. We found that the vast majority of ventricular CMs in rapidly growing fish were mononucleate (95.6%), as were CMs from fish kept at SG (97.9%) and MS conditions (95.1%), indicating derivation through cytokinesis (Fig. 2D,E). Thus, homeostatic cardiac growth and maintenance are primarily the result of bona fide CM hyperplasia, with the vigor of this hyperplasia dependent on the rate of animal growth.

Evidence that myocardial homeostasis is aided by progenitor cells

Homeostatic CM generation must occur through the division of mature CMs, or the maturation of myocardial progenitor cells, or both. During regeneration, cells expressing markers of embryonic cardiac progenitor cells such as *hand2* (Yelon et al., 2000) are established at the apical edge of the wounded muscle within 3-4 days

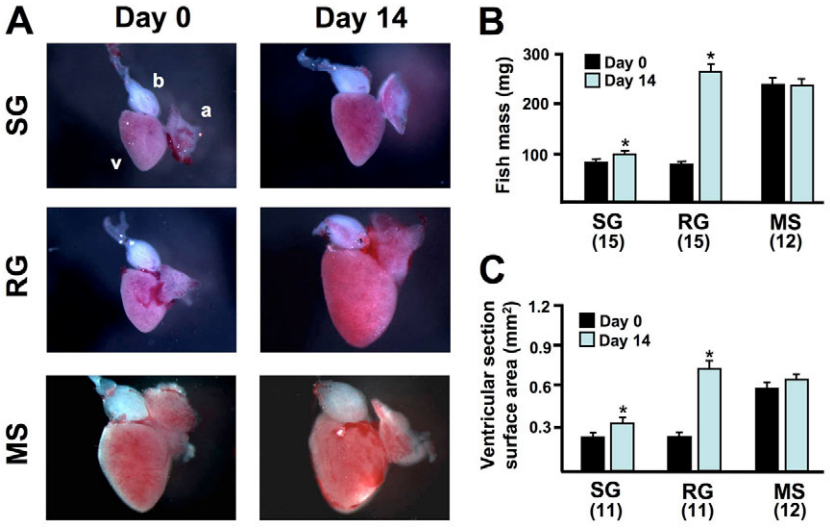

Fig. 1. Experimental control of animal and cardiac growth in adult zebrafish.
(**A**) Representative images of hearts collected from animals maintained for 14 days in conditions for rapid growth (RG), slow growth (SG) or to maintain size (MS). Hearts in images may be missing some atrial tissue lost during tissue collection. a, atrium; b, bulbous arteriosus v, ventricle. (**B**) Quantification of animal mass of RG, SG and MS fish. RG fish had a much higher increase in body mass from day 0 than their SG clutchmates at day 14, whereas MS fish maintained mass (*P<0.001, t-test, significantly different from day 0). The numbers of animals per group are shown in parentheses. (**C**) Quantification of ventricular size in RG, SG and MS fish. Ventricles in the RG group showed much greater size increases than those of SG clutchmates at day 14, while ventricular size remained stable in MS fish (*P<0.005, t-test, significantly different from day 0).

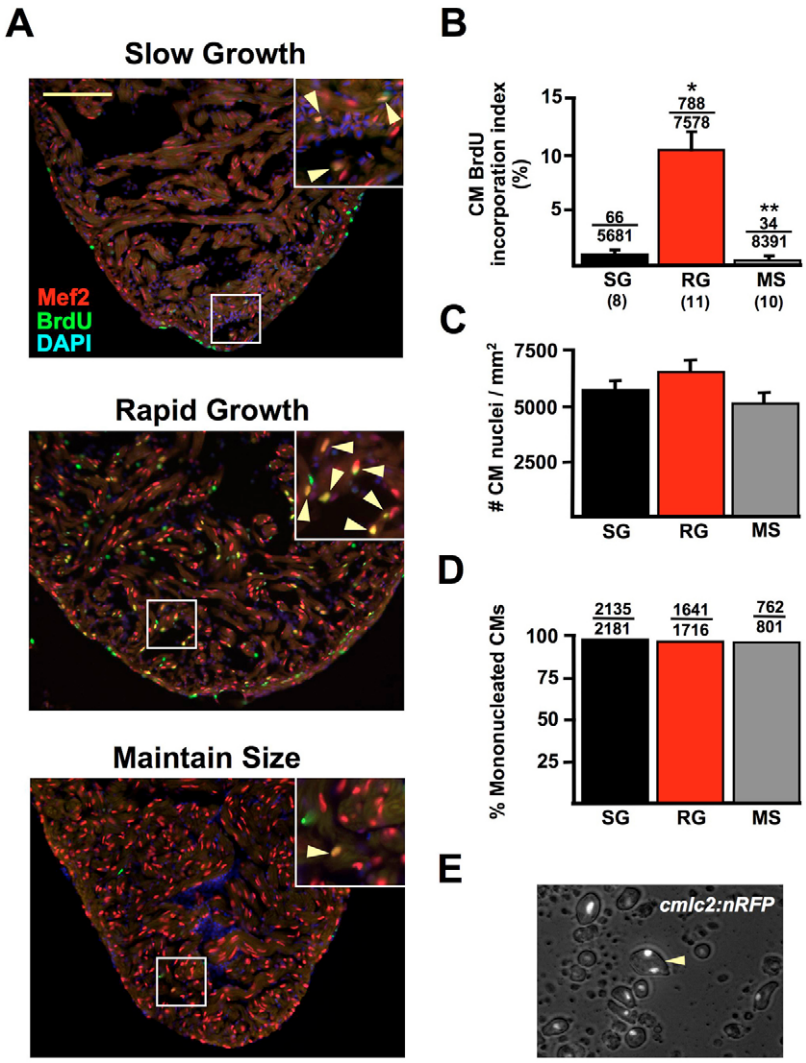

Fig. 2. Cardiac homeostasis involves cardiomyocyte hyperplasia. (**A**) Ventricles from SG, RG and MS animals stained for Mef2 expression to identify CMs (red), and for BrdU incorporation (green). CM BrdU incorporation was much greater in RG ventricles (arrowheads in insets). Nuclei are labeled with DAPI (blue). (**B**) Quantification of CM BrdU incorporation in SG, RG and MS groups, plotted as the average BrdU incorporation index per animal (*P<0.001, t-test, significantly different from SG; **P<0.05, t-test, significantly different from SG and RG). Numbers above the error bars indicate BrdU-positive CMs over the total CMs counted from all animals combined. Numbers below group abbreviations indicate the number of animals/ventricles per group. (**C**) CM hypertrophy was assessed by measuring the number of Mef2-positive nuclei per area of myocardium, as described in Materials and methods. No significant differences in CM density were observed between RG ventricles (6540±505 CMs/mm^2) and SG (5842±326 CMs/mm^2) or MS ventricles (5167±422 CMs/mm^2). Eight animals were used per group. (**D**) Quantification of nuclei in CMs dissociated from pooled *cmlc2:nRFP* ventricles from different homeostatic conditions, indicating that 97.9% of CMs are mononucleate in SG ventricles, 95.6% in RG ventricles and 95.1% in MS ventricles. (**E**) Image of dissociated ventricular CMs (cells with white nuclei) from *cmlc2:nRFP* animals. Binucleated myocytes (arrowhead) are rare in adult zebrafish under RG, SG, or MS conditions. Thus, CM hypertrophy and binucleation play little or no role in homeostatic cardiac growth. Scale bar in A: 100 μm.

post injury, and are maintained at that edge as regeneration progresses (Lepilina et al., 2006). The origin of these cells is unknown; they might exist as resident non-myocardial cells activated upon injury, or be created through reduction in contractile function of existing CMs, known as de-differentiation. Strong, discrete *hand2* in situ hybridization signals analogous to that seen during myocardial regeneration were common in RG animals particularly within the compact myocardium, sparingly present in SG animals, and largely absent in MS adults (Fig. 3A). Real-time quantitative PCR experiments indicated that *hand2* expression in RG ventricles was 1.4 fold that of SG clutchmates, and 2.5 fold that of MS ventricles (Fig. 3C).

hand2 is expressed in embryonic progenitors but is not a definitive marker of undifferentiated cells. To test the idea that progenitor cell populations give rise to new CMs during homeostasis, we assessed CM maturation in the *cmlc2:nRFP* transgenic line, a strain that reports a slow-folding, nuclear-localized DsRed2 protein under control of the *cardiac myosin light chain 2* (*myl7* – Zebrafish Information Network) promoter (Mably et al., 2003). Mature CMs in these transgenic fish show nuclear-localized DsRed fluorescence. However, an anti-DsRed antibody detects unfolded, cytosolic DsRed fluorescence in the new CMs of the 24-hour post-fertilization embryo and the regenerating edge of the injured adult ventricle, apparently before nuclear localization occurs and natural fluorescence is manifest. Thus, this marker (RFP^{cyto}) appears to serve as an indicator of developmental transition from undifferentiated progenitor cells to differentiated CMs (Lepilina et al., 2006). We found that 10.7±2.1% of CMs throughout the ventricle of RG animals expressed the RFP^{cyto} marker, a percentage over three times that of SG clutchmates (3.1±0.3%) and 36 times that of MS fish (0.3±0.1%; Fig. 3B,D). In ventricles of *cmlc2:nRFP* RG animals that had been injected with BrdU, both RFP^{cyto} and RFP^{nuc} CMs showed BrdU-labeled nuclei, suggesting that both the most recently maturing CMs and earlier-maturing CMs undergo proliferation (data not shown). In total, these results suggest that myocardial progenitor cell populations contribute at least in part to the vigorous generation of new CMs stimulated by rapid animal growth, and in rare events during homeostatic maintenance of heart size.

Homeostatic developmental activation of the adult epicardium

During zebrafish heart regeneration, local injury strongly activates expression of the embryonic epicardial markers *raldh2* and *tbx18* throughout the entire ventricular and atrial epicardium. This activation is accompanied by epicardial cell proliferation, expanding the epithelial cover of the ventricle to eventually cover the injury (Lepilina et al., 2006). *raldh2* and *tbx18* were expressed at low levels

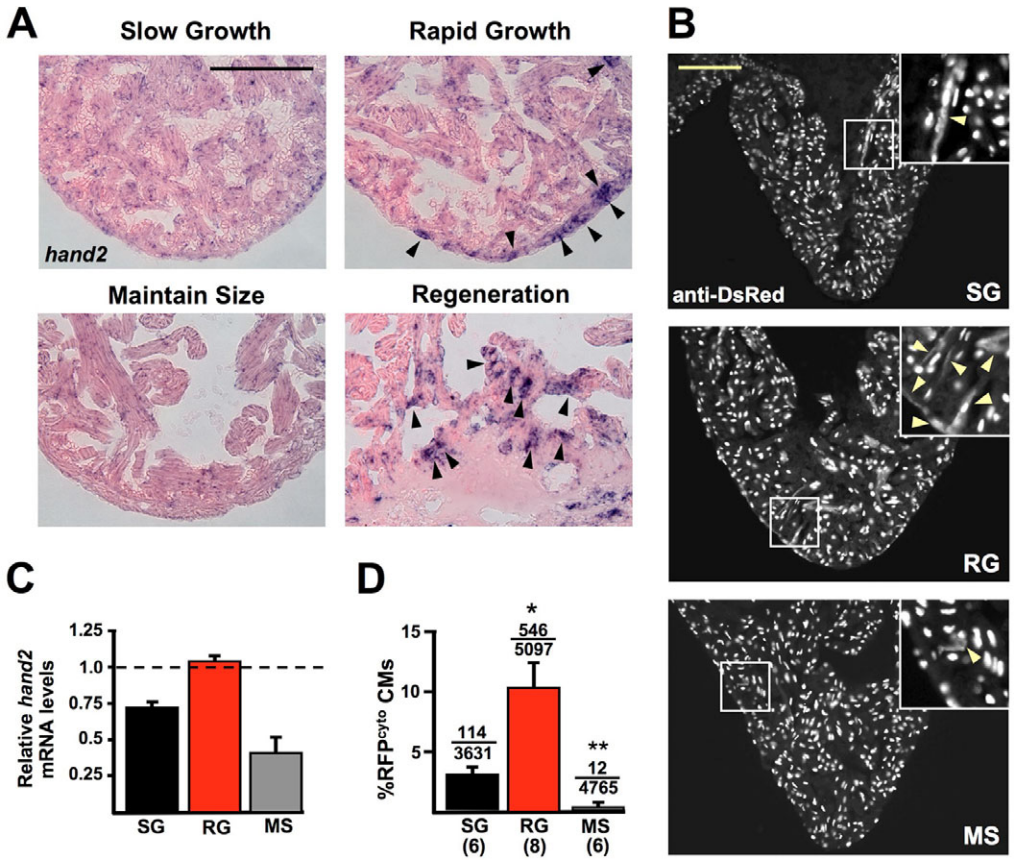

Fig. 3. Cardiogenic markers are induced during cardiac homeostasis. (**A**) *hand2* in situ hybridization of ventricular sections. *hand2* is weakly expressed in MS hearts, mildly expressed in SG hearts and more strongly expressed in RG hearts similar to regenerating hearts 7 days post-resection (arrowheads show foci of strong expression). (**B**) Sections from SG, RG and MS ventricles of *cmlc2:nRFP* zebrafish, stained for DsRed immunoreactivity. RG ventricles show many more RFP^{cyto} cells, a marker that suggests recent CM differentiation events (arrowheads in insets). (**C**) Real-time Q-PCR analysis of *hand2* expression from whole ventricles of SG, RG and MS hearts, relative to expression in ventricles 7 days after apical resection. *hand2* expression is similar in ventricles from RG fish to that in regenerating ventricles (1.0, represented by dashed line) and greater than in SG and MS ventricles. (**D**) Quantification of RFP^{cyto} cells in SG, RG and MS groups. The average RFP^{cyto} index per animal is plotted. Numbers above the error bars indicate RFP^{cyto} CMs over the total CMs counted from all animals combined. Numbers below group abbreviations indicate the number of animals/ventricles per group (*P<0.01, *t*-test, significantly different from SG; **P<0.005, *t*-test, significantly different from SG and RG). Scale bars: 100 μm.

in a small number of epicardial cells in both SG and MS ventricles, indicating moderate activation. By contrast, these markers were robustly induced in contiguous stretches of RG atrial and ventricular epicardium (Fig. 4A, Fig. 5B). In addition, endocardial cells surrounding cardiac myofibers near the injury site have been shown to induce *raldh2* during regeneration (R.J.M. and K.D.P., unpublished) (Lepilina et al., 2006). We found that RG animals, but not SG or MS animals, displayed strong *raldh2* expression in endocardial cells throughout the ventricle (arrows in Fig. 4A; A.A.W., J.E.H. and K.D.P., unpublished). Thus, embryonic gene expression within both the epicardium and endocardium is activated by rapid animal growth.

We suspected that, because of its location and exquisite sensitivity to growth and injury, the epicardium may act as a sensor to identify changes in animal growth through sensation of pressure changes in the extra-cardiac space. The pericardial sac is filled with a plasma ultrafiltrate that is believed to have a restrictive function during diastole. Therefore, opening the cavity might relieve pressure, increasing cardiac stretch. Conversely, saline injection is expected to increase pericardial pressure and limit the ability of the heart to expand (Farrell et al., 1988; Shabetai et al., 1985; Spodick, 1997). To test whether these procedures affect epicardial gene expression, we examined *raldh2* expression in several groups of experimentally manipulated 6-month-old MS animals. We found that ventricular *raldh2* expression was induced to roughly the same level as in RG animals (but at levels lower than after partial ventricular resection) in experiments in which (1) the pericardial sac was surgically opened, or (2) saline was carefully injected into the pericardial cavity (Fig. 4B). Different manipulations that resulted in no effect on epicardial *raldh2* expression included: (1) piercing the pericardial sac without saline injection, (2) lesions to the dorsal region of the animal and (3) fin amputation. These results show that the epicardium is a dynamic tissue responsive to changes in the milieu surrounding the heart, and suggest that the effects of rapid animal growth on epicardial gene expression are due in part to an ability of the epicardial tissue to sense changes in resistance within the extra-cardiac space.

Epicardial-derived cells recurrently supplement the ventricular wall

During embryonic heart development, a subset of epicardial cells undergoes epithelial-mesenchymal transition (EMT) and migrates into the underlying subepicardial space and myocardial wall as

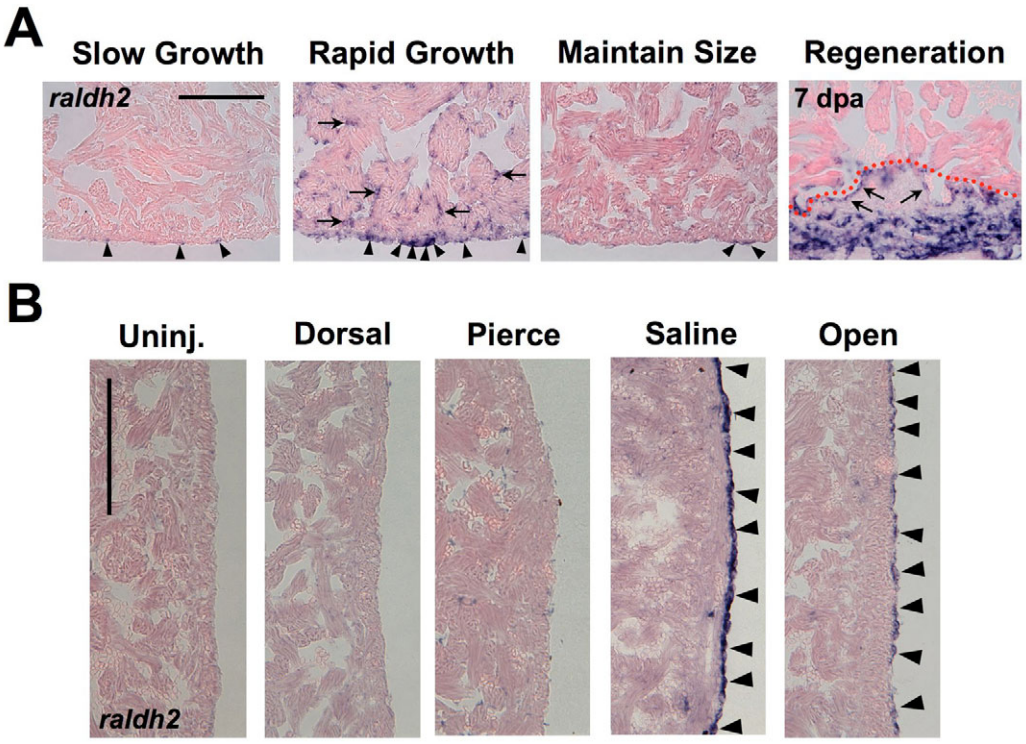

Fig. 4. Developmental activation of the epicardium in response to growth or manipulation of the extracardiac environment. (**A**) Ventricles from SG, RG, or MS animals stained for *raldh2* expression. *raldh2* is weakly expressed in rare cells of SG and MS epicardia (arrowheads), but strongly expressed in epicardial cells of RG hearts, similar to the expression seen at the wound at 7 days post-amputation (right). Ventricular endocardial cells surrounding inner trabecular myofibers also induced *raldh2* during rapid growth, similar to induction during regeneration (arrows in RG and Regeneration). (**B**) Assessment of *raldh2* expression in ventricular epicardium 3 days after different manipulations in 6-month-old MS animals (lateral ventricular wall is shown). Surgically opening the pericardial sac (Open) or injecting saline into the pericardial sac (Saline) stimulated *raldh2* expression (arrowheads), whereas injuries to the dorsal side of the animal (Dorsal), or piercing the pericardial sac with an empty needle (Pierce) did not. Scale bars: 100 μm.

epicardial-derived cells (EPDCs). There, EPDCs contribute fibroblasts as well as smooth muscle and/or endothelial cells for building coronary vasculature (Olivey et al., 2004; Reese et al., 2002). To determine whether the adult zebrafish epicardium actively transfers cells subepicardially to the ventricular wall, we performed a pulse-chase experiment. We labeled the epicardium by filling the pericardial sac of MS zebrafish with the fluorescent lipophilic dye DiI, and then harvested hearts at different timepoints post-injection. Dye was limited to the epicardium at 1 hour post-injection; by contrast, we noticed a small number of labeled cells separated from the epicardium by 3 days post-injection. Occasionally, these labeled cells had a tubular morphology reminiscent of vascular tissue (inset, Fig. 5A). At 7 and 14 days post-injection, DiI was concentrated in cells that were embedded within the otherwise unlabeled ventricular wall inward from the now faintly labeled epicardium (Fig. 5A). Interestingly, labeled cells occasionally appeared to constitute a distinct layer of 15-20 μm at the junction of compact and trabecular myocardium. These surprising data indicate that the adult epicardium is a dynamic tissue that regularly contributes EPDCs to the ventricular wall, presumably through EMT.

Applying labeled dye to the pericardium elevated epicardial expression of *raldh2* similar to saline injection (data not shown), implying that this treatment induces strong developmental activation of the epicardium and likely affected its contributions to the ventricular wall. To evaluate EPDC activity in unmanipulated animals, we utilized the embryonic epicardial marker *tbx18*. During regeneration, cells positive for the embryonic epicardial marker *tbx18* emerge not only in the epicardium, but in subepicardial tissue within the wound and regenerating muscle (Lepilina et al., 2006). Interestingly, in uninjured ventricles, *tbx18*-expressing cells were also present both in the epicardium and several cell layers deep into the compact myocardium. Many *tbx18*-positive cells were located in what appeared as a distinct layer 15-20 μm subepicardially, a location similar to the EPDCs revealed by our pulse-chase experiments (Fig. 5B). For these reasons, we inferred that *tbx18* is a robust marker for emergent EPDCs in the uninjured ventricular wall. Quantification of these internalized *tbx18*-positive EPDCs revealed that the density of EPDCs in RG animals was almost six times as high as in SG animals (27.4±1.6 vs 4.9±1.0 *tbx18*-positive cells/mm ventricular wall). Somewhat unexpectedly, MS animals had more than twice as many *tbx18*-positive EPDCs as SG animals (11.9±1.8; Fig. 5C). This may be a consequence of age differences between these groups, and/or the possibility that *tbx18* is a cumulative marker of EPDCs that have emerged in the ventricular wall over weeks to months. The latter idea is supported by the observation that regenerated muscle possesses cells robustly expressing *tbx18* for 30 days or more after injury (Lepilina et al., 2006). Given the role of epicardial tissue during embryonic heart growth and the appearance of *tbx18*-positive cells coincident with new vascular tissue during regeneration, we postulate that *tbx18*-positive EPDCs contribute to neovascularization of emergent myocardial tissue and/or vascular maintenance in uninjured animals. Indeed, we could observe in some cases cells positive for *tbx18* that had the appearance of vascular tissue (Fig. 5B, red arrowhead and inset), similar to DiI-

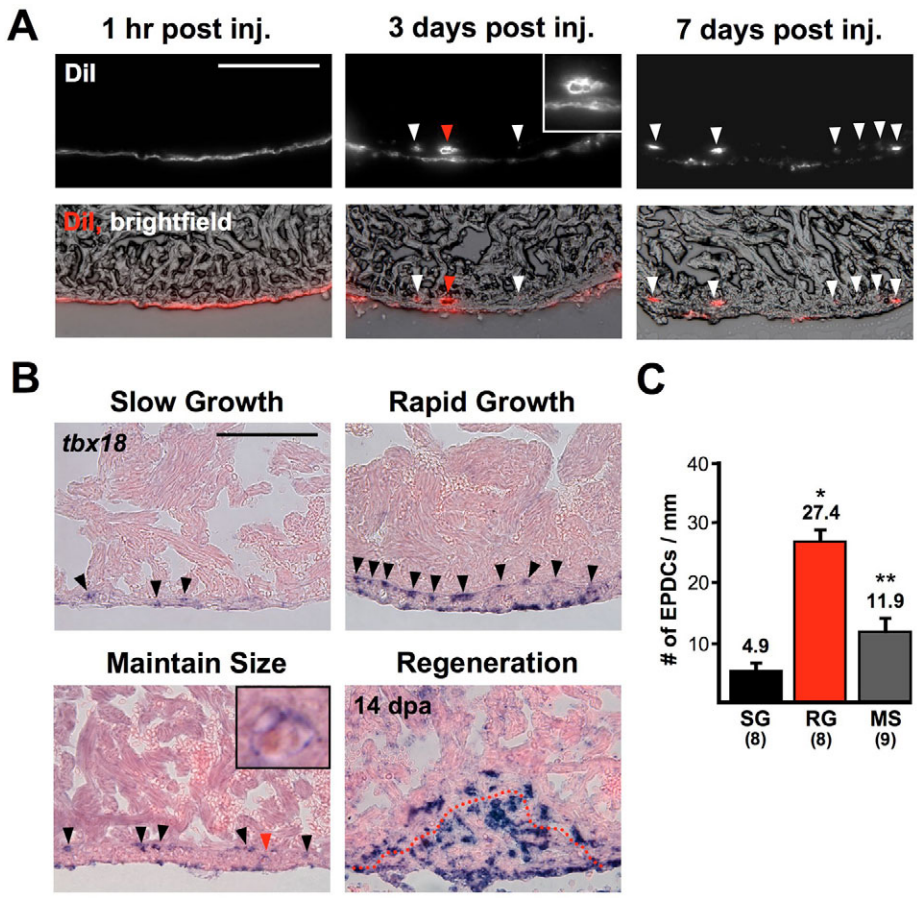

Fig. 5. Contribution of epicardial-derived cells (EPDCs) to the ventricular wall. (**A**) DiI was carefully injected into the pericardial sac to label the epicardium, and hearts were collected at 1 hour, 3 days and 7 days post-injection. Dye is restricted to epicardial cells at 1 hour, but at 3 days EPDCs are occasionally seen in the compact layer (arrowheads). The red arrow indicates labeled tissue with the appearance of vascular tissue (enlarged in the inset). By 7 days post-injection, DiI-containing EPDCs are observed deep in the ventricular wall, with less label within the epicardial layer. Many of these cells appear to contribute to an inner layer of labeled cells ~15-20 μm into the wall. (**B**) *tbx18* is expressed in many more epicardial cells and EPDCs (arrowheads) in RG animals than in other groups. (Inset) Enlarged image of area indicated by the red arrowhead: some *tbx18*-positive EPDCs within the ventricle showed a morphology characteristic of vascular cells. The red dotted line in injured animals indicates the border between myocardium and clot material. (**C**) Quantification of *tbx18*-positive EPDCs from SG, RG and MS ventricles. (*P<0.001, *t*-test, significantly different from SG; **P<0.01, *t*-test, significantly different from RG and SG). Scale bars: 100 μm.

labeled cells in pulse-chase experiments. Thus, the adult epicardium supports cardiac homeostasis by regular contribution of new EPDCs to the ventricular wall.

Cardiac homeostasis requires Fibroblast growth factor signaling

Recent studies have revealed roles for Fgfs in epicardial EMT during both embryonic heart development and adult heart regeneration. EMT of cultured embryonic epicardial cells can be stimulated by Fgfs in vitro, and this pathway is necessary for normal coronary vascular development in mice (Lavine et al., 2006; Morabito et al., 2001). During zebrafish heart regeneration, the injured zebrafish myocardium increases expression of *fgf17b*, while the receptors *fgfr2* and *fgfr4* are expressed in EPDCs. Furthermore, abrogation of Fgf signaling disrupts EPDC supplementation of the wound and new muscle during regeneration, inhibiting neovascularization and myocardial renewal (Lepilina et al., 2006). We found that *fgf17b*, *fgfr2* and *fgfr4* were all present in SG and RG ventricles, although no differences in expression between the two groups were detectable by in situ hybridization (data not shown). Based on these findings, we suspected that Fgf signaling may also be important for EPDC supplementation of the ventricle during cardiac homeostasis.

To test this idea, we placed zebrafish transgenic for a heat-inducible dominant-negative Fgf receptor (*hsp70:dn-fgfr1*) and their wild-type clutchmates in RG conditions for 14 days, and applied a daily heat-shock (Lee et al., 2005). Transgenic animals appeared healthy during the experiment, although they grew less than wild-type animals under RG conditions (see Fig. S3 in the supplementary material). Although *tbx18* expression was comparable between transgenics and wild types in the epicardium itself, the density of *tbx18*-positive EPDCs within the ventricular walls of *hsp70:dn-fgfr1* animals was less than half that in wild-type animals (Fig. 6A,B; 24.6±2.1 EPDCs/mm in wild type, versus 11.5±2.1, in *hsp70:dn-fgfr1*). Fgfr inhibition also resulted in a slight reduction in ventricular growth under RG conditions, with transgenic animals exhibiting ~31% less of a growth increase than wild-type clutchmates (Fig. 6C). Thus, normal homeostatic supplementation of the ventricular wall by EPDCs requires Fgf signaling. We suspect that the partial phenotype is due to the continued presence of other factors that act on EPDCs, incomplete inhibition of Fgf signaling, and/or the possibility mentioned above that *tbx18* expression reflects cumulative events of EPDC contribution.

As pulse-chase and *tbx18* expression experiments indicated ongoing EPDC contribution even in the absence of significant cardiac growth, we tested the requirements for Fgf signaling in mature adult zebrafish. We delivered a long-term block of Fgf signaling by daily heat-shocks to *hsp70:dn-fgfr1* transgenics for 60-70 days, with identical heat-shocks given to wild-type clutchmates. We found that ~15% of *hsp70:dn-fgfr1* fish developed extensive collagen deposition within the ventricular wall after this period, indicating the presence of scar tissue (Fig. 6D; n=39 fish). No wild-type animals displayed scarring (n=44 fish; Fisher-Irwin test, P<0.01). We suspect that these fibrotic events resulted from reduced efficiency of incremental EPDC supplementation over the 2-month period, although marker examination revealed no obvious defects (data not shown). These results demonstrate that Fgf signaling is essential for normal homeostatic growth and maintenance of cardiac tissue in the adult zebrafish.

DISCUSSION

Hyperplastic myocardial and epicardial homeostasis in the adult zebrafish ventricle

We have discovered that new myocardial and epicardial-derived cells are created during homeostatic responses of the adult zebrafish heart, helping to couple cardiac and animal growth rate and maintain cardiac integrity. One molecular signaling pathway essential for these responses is that mediated by Fgfs, which ensures normal supplementation of the ventricular wall with EPDCs and helps to prevent scarring.

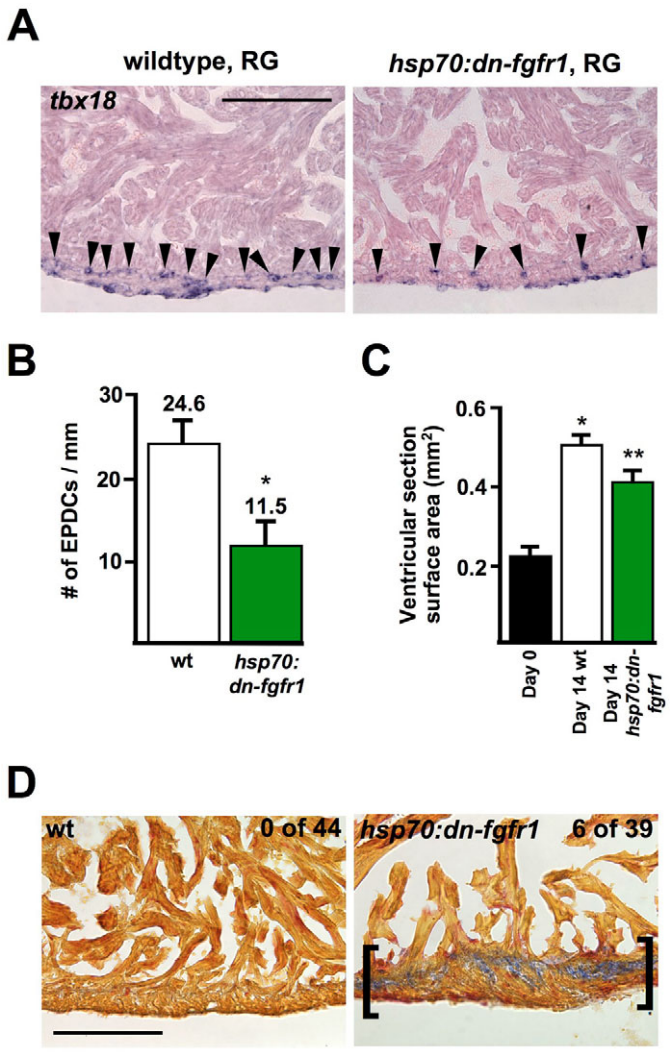

Fig. 6. Fgf signaling is required for cardiac homeostasis. (**A**,**B**) *tbx18* expression in ventricles of wild-type and *hsp70:dn-fgfr1* transgenic zebrafish after 14 days RG conditions, with a single daily heat-shock. Although epicardial expression is comparable, significantly fewer EPDCs (arrowheads) are observed within *hsp70:dn-fgfr1* ventricular walls (*P<0.001, *t*-test, n=10). (**C**) Fgfr inhibition attenuates ventricular growth of RG fish (*P<0.001, *t*-test, significantly different from day 0; **P<0.01, *t*-test, significantly different from day 0 and from day 14 wild type, n=9). Day 0 measurements are the results of pooled transgenics and wild types. (**D**) Acid-fuschin-Orange G staining (AFOG) on ventricles of wild-type and *hsp70:dn-fgfr1* animals after 60-70 days of daily heat-shocks. Scars (brackets) were observed in ~15% of uninjured transgenic fish (n=39), but never observed in wild-type clutchmates given the same daily heat-shock protocol (n=44) (P<0.01, Fisher-Irwin exact test). Scale bars: 100 μm.

In contrast to what is known about postnatal ventricular growth in mammals, we have found that cardiac growth in zebrafish is a result of CM proliferation, not the hypertrophy of existing cells. Ventricular expression of the embryonic progenitor marker *hand2*, as well as a transitional marker for newly generated cardiomyocytes in *cmlc2:nRFP* transgenic fish, showed positive correlations with cardiac growth and CM proliferation. Thus, these results suggest that undifferentiated progenitor cells contribute to CM hyperplasia. Future experiments to address the extent to which this occurs must involve genetic fate-mapping strategies (Cai et al., 2003; Dor et al., 2004; Hsieh et al., 2007; Meilhac et al., 2003). Moreover, it will be critical to define homeostatic signals that trigger cardiomyogenesis and how these signals are distributed and calibrated in the adult animal.

As a thin epithelium covering the entire surface of the heart, the epicardium has an ideal architecture for relaying such homeostatic signals. Numerous studies support this idea, because: (1) the epicardium serves as a source of mitogens in the embryonic heart (Chen et al., 2002; Merki et al., 2005; Reese et al., 2002), (2) organ-wide developmental gene expression is activated within the adult zebrafish epicardium within hours of cardiac injury (Lepilina et al., 2006), and (3) during regenerative cardiogenesis as well as homeostatic cardiac growth, developmentally active epicardium is present at sites of cardiogenesis (Lepilina et al., 2006). Indeed, consistent with this idea are the findings here that manipulations of the pericardial environment that mimic growth-induced changes in pericardial space cause epicardial responses similar to those elicited by homeostatic growth. Because epicardial retinoic acid (RA) synthesis is regulated in each of these scenarios and is known to influence CM proliferation in embryos (Chen et al., 2002; Stuckmann et al., 2003), this molecule is a strong candidate for homeostatic regulation of cardiogenesis. We have found that the endocardium also increases RA synthesis during adult growth and regeneration. It is possible that endocardial cell activity regulates growth and/or remodeling of the inner trabecular muscle, which would appear to have reduced access to epicardial signaling molecules.

In addition to serving as a source of RA, we found that the epicardium also regularly contributes cells to the compact myocardial wall of the ventricle. Thus, the epicardium is by no means a static tissue in adult animals, but rather one that actively sustains the ventricle. This conclusion is bolstered by our finding that sustained inhibition of Fgf signaling, which disrupts EPDC supplementation in rapidly growing fish, led to spontaneous scar formation in animals maintaining their animal and organ size. Further exploration of the fate and function of these adult EPDCs, using tissue-specific fate-mapping and ectopic expression tools, will illuminate the roles of the epicardium in cardiac homeostasis. From what is known of embryonic heart development, it is likely that the adult zebrafish myocardial wall requires new EPDCs to replenish vasculature, or to neovascularize newly created muscle, or both. It will also be fascinating to learn to what extent the epicardium participates in homeostasis of the adult mammalian ventricular wall.

Cardiac growth, maintenance and regeneration

Our study exposes important similarities between cardiac homeostasis and cardiac regeneration. In each case, new myocardial and epicardial-derived tissues are generated in amounts appropriate to animal size, involving expression of a suite of cardiogenic developmental markers. Whereas regeneration is characterized by an intense focus of cardiogenesis at the injury site, homeostasis

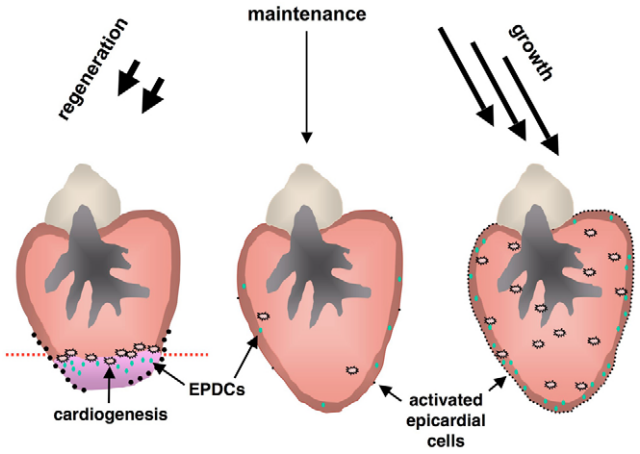

Fig. 7. Model for cardiac homeostasis in zebrafish. Regeneration, maintenance and growth share cardiogenic signaling pathways (black arrows above ventricles) to generate new CMs and EPDCs in adult zebrafish. Regeneration involves developmental activation of the epicardium (black dots) and local recruitment of EPDCs to a focus of new CM production (pink explosions) at the wound (red dotted line). For simplicity, a cartoon of the ventricle at 7 dpa is shown, after the epicardial response has localized to the injury site. In the uninjured MS ventricle (maintenance), CM generation, epicardial activation and EPDC recruitment are diffuse and rare to counter occasional cell loss events. During rapid animal growth (growth), robust chamber-wide increases in CM generation, epicardial activation and EPDC mobilization are stimulated. Thus, similar or identical cardiogenic pathways are regulated with different intensities and localization to facilitate cardiac regeneration, maintenance or growth in adult zebrafish.

involves organ-wide cell addition in doses dependent on the vigor of animal growth. Thus, the adult zebrafish not only has the ability to generate new cardiac tissues, but can also control the intensity and the spatial distribution of these cardiogenic events to select replacement of a portion of tissue, rapid chamber-wide growth, or occasional exchange of a few cells (Fig. 7).

This relationship between cardiac regeneration, homeostatic growth and homeostatic tissue maintenance is likely to be important for explaining why zebrafish regenerate injured cardiac muscle. Both regeneration and homeostasis stand to benefit from sophisticated mechanisms to activate and deploy epicardial and myocardial cells for cardiogenesis. In some teleosts, adult growth rate is controlled by environmental and/or social factors and can influence mating preference (Borowsky, 1973; Hofmann et al., 1999). Thus, one reason why cardiac regeneration persists in zebrafish, and probably other teleosts, may be the accessibility of injured tissue to cellular and molecular machinery that is normally employed for rapid indeterminate growth. This notion makes sense in light of extremely weak hyperplasia in the injured or uninjured hearts of adult mammals, species with determinate growth. Continued study of cardiac regeneration and homeostasis in zebrafish, including comparisons with mammalian cardiac dynamics, will expose critical mechanisms by which cardiac tissues are rejuvenated.

We thank A. Lepilina for TUNEL assays, C. Wheeler, O. Ighile, C. Parobek, J. Bumgardner and T. Yu for excellent fish care, A. Nechiporuk, S. Odelberg, and lab members for helpful comments on the manuscript. R.J.M. was supported by NIH training grant 2 T-32 HL007101-31. This work was supported by grants to K.D.P. from NHLBI, American Heart Association, Whitehead Foundation, and Pew Charitable Trusts.

Supplementary material

Supplementary material for this article is available at
http://dev.biologists.org/cgi/content/full/135/1/183/DC1

References

Beltrami, A. P., Barlucchi, L., Torella, D., Baker, M., Limana, F., Chimenti, S., Kasahara, H., Rota, M., Musso, E., Urbanek, K. et al. (2003). Adult cardiac stem cells are multipotent and support myocardial regeneration. *Cell* **114**, 763-776.

Borowsky, R. L. (1973). Social control of adult size in males of *Xiphophorus variatus*. *Nature* **245**, 332-335.

Cai, C. L., Liang, X., Shi, Y., Chu, P. H., Pfaff, S. L., Chen, J. and Evans, S. (2003). Isl1 identifies a cardiac progenitor population that proliferates prior to differentiation and contributes a majority of cells to the heart. *Dev. Cell* **5**, 877-889.

Chen, T. H., Chang, T. C., Kang, J. O., Choudhary, B., Makita, T., Tran, C. M., Burch, J. B., Eid, H. and Sucov, H. M. (2002). Epicardial induction of fetal cardiomyocyte proliferation via a retinoic acid-inducible trophic factor. *Dev. Biol.* **250**, 198-207.

Conlon, I. and Raff, M. (1999). Size control in animal development. *Cell* **96**, 235-244.

Dor, Y., Brown, J., Martinez, O. I. and Melton, D. A. (2004). Adult pancreatic beta-cells are formed by self-duplication rather than stem-cell differentiation. *Nature* **429**, 41-46.

Farrell, A. P., Johanson, J. A. and Graham, M. S. (1988). The role of the pericardium in cardiac performance of the trout (*Salmo gairdneri*). *Physiol. Zool.* **61**, 213-221.

Flink, I. L. (2002). Cell cycle reentry of ventricular and atrial cardiomyocytes and cells within the epicardium following amputation of the ventricular apex in the axolotl, Amblystoma mexicanum: confocal microscopic immunofluorescent image analysis of bromodeoxyuridine-labeled nuclei. *Anat. Embryol.* **205**, 235-244.

Hofmann, H. A., Benson, M. E. and Fernald, R. D. (1999). Social status regulates growth rate: consequences for life-history strategies. *Proc. Natl. Acad. Sci. USA* **96**, 14171-14176.

Hsieh, P. C., Segers, V. F., Davis, M. E., Macgillivray, C., Gannon, J., Molkentin, J. D., Robbins, J. and Lee, R. T. (2007). Evidence from a genetic fate-mapping study that stem cells refresh adult mammalian cardiomyocytes after injury. *Nat. Med.* **13**, 970-974.

Jordan, D. S. (1905). *A Guide to the Study of Fishes*. New York: Henry Holt.

Laugwitz, K. L., Moretti, A., Lam, J., Gruber, P., Chen, Y., Woodard, S., Lin, L. Z., Cai, C. L., Lu, M. M., Reth, M. et al. (2005). Postnatal isl1+ cardioblasts enter fully differentiated cardiomyocyte lineages. *Nature* **433**, 647-653.

Lavine, K. J., White, A. C., Park, C., Smith, C. S., Choi, K., Long, F., Hui, C. C. and Ornitz, D. M. (2006). Fibroblast growth factor signals regulate a wave of Hedgehog activation that is essential for coronary vascular development. *Genes Dev.* **20**, 1651-1666.

Lee, Y., Grill, S., Sanchez, A., Murphy-Ryan, M. and Poss, K. D. (2005). Fgf signaling instructs position-dependent growth rate during zebrafish fin regeneration. *Development* **132**, 5173-5183.

Lepilina, A., Coon, A. N., Kikuchi, K., Holdway, J. E., Roberts, R. W., Burns, C. G. and Poss, K. D. (2006). A dynamic epicardial injury response supports progenitor cell activity during zebrafish heart regeneration. *Cell* **127**, 607-619.

Li, F., Wang, X., Capasso, J. M. and Gerdes, A. M. (1996). Rapid transition of cardiac myocytes from hyperplasia to hypertrophy during postnatal development. *J. Mol. Cell. Cardiol.* **28**, 1737-1746.

Mably, J. D., Mohideen, M. A., Burns, C. G., Chen, J. N. and Fishman, M. C. (2003). heart of glass regulates the concentric growth of the heart in zebrafish. *Curr. Biol.* **13**, 2138-2147.

Martin, C. M., Meeson, A. P., Robertson, S. M., Hawke, T. J., Richardson, J. A., Bates, S., Goetsch, S. C., Gallardo, T. D. and Garry, D. J. (2004). Persistent expression of the ATP-binding cassette transporter, Abcg2, identifies cardiac SP cells in the developing and adult heart. *Dev. Biol.* **265**, 262-275.

Meilhac, S. M., Kelly, R. G., Rocancourt, D., Eloy-Trinquet, S., Nicolas, J. F. and Buckingham, M. E. (2003). A retrospective clonal analysis of the myocardium reveals two phases of clonal growth in the developing mouse heart. *Development* **130**, 3877-3889.

Merki, E., Zamora, M., Raya, A., Kawakami, Y., Wang, J., Zhang, X., Burch, J., Kubalak, S. W., Kaliman, P., Belmonte, J. C. et al. (2005). Epicardial retinoid X receptor alpha is required for myocardial growth and coronary artery formation. *Proc. Natl. Acad. Sci. USA* **102**, 18455-18460.

Molkentin, J. D. and Markham, B. E. (1993). Myocyte-specific enhancer-binding factor (MEF-2) regulates alpha-cardiac myosin heavy chain gene expression in vitro and in vivo. *J. Biol. Chem.* **268**, 19512-19520.

Morabito, C. J., Dettman, R. W., Kattan, J., Collier, J. M. and Bristow, J. (2001). Positive and negative regulation of epicardial-mesenchymal transformation during avian heart development. *Dev. Biol.* **234**, 204-215.

Oberpriller, J. O. and Oberpriller, J. C. (1974). Response of the adult newt ventricle to injury. *J. Exp. Zool.* **187**, 249-253.

Oh, H., Bradfute, S. B., Gallardo, T. D., Nakamura, T., Gaussin, V., Mishina, Y., Pocius, J., Michael, L. H., Behringer, R. R., Garry, D. J. et al. (2003).

Cardiac progenitor cells from adult myocardium: homing, differentiation, and fusion after infarction. *Proc. Natl. Acad. Sci. USA* **100**, 12313-12318.
Olivey, H. E., Compton, L. A. and Barnett, J. V. (2004). Coronary vessel development: the epicardium delivers. *Trends Cardiovasc. Med.* **14**, 247-251.
Poss, K. D., Wilson, L. G. and Keating, M. T. (2002). Heart regeneration in zebrafish. *Science* **298**, 2188-2190.
Potter, C. J. and Xu, T. (2001). Mechanisms of size control. *Curr. Opin. Genet. Dev.* **11**, 279-286.
Reese, D. E., Mikawa, T. and Bader, D. M. (2002). Development of the coronary vessel system. *Circ. Res.* **91**, 761-768.
Shabetai, R., Abel, D. C., Graham, J. B., Bhargava, V., Keyes, R. S. and Witztum, K. (1985). Function of the pericardium and pericardioperitoneal canal in elasmobranch fishes. *Am. J. Physiol.* **248**, H198-H207.
Smart, N., Risebro, C. A., Melville, A. A., Moses, K., Schwartz, R. J., Chien, K. R. and Riley, P. R. (2007). Thymosin beta4 induces adult epicardial progenitor mobilization and neovascularization. *Nature* **445**, 177-182.
Soonpaa, M. H. and Field, L. J. (1997). Assessment of cardiomyocyte DNA synthesis in normal and injured adult mouse hearts. *Am. J. Physiol.* **272**, H220-H226.
Soonpaa, M. H., Kim, K. K., Pajak, L., Franklin, M. and Field, L. J. (1996). Cardiomyocyte DNA synthesis and binucleation during murine development. *Am. J. Physiol.* **271**, H2183-H2189.
Spodick, D. H. (1997). *The Pericardium: A Comprehensive Textbook*. New York: Marcel Dekker.
Stuckmann, I., Evans, S. and Lassar, A. B. (2003). Erythropoietin and retinoic acid, secreted from the epicardium, are required for cardiac myocyte proliferation. *Dev. Biol.* **255**, 334-349.
Taub, R. (2004). Liver regeneration: from myth to mechanism. *Nat. Rev. Mol. Cell Biol.* **5**, 836-847.
Tsai, S. B., Tucci, V., Uchiyama, J., Fabian, N. J., Lin, M. C., Bayliss, P. E., Neuberg, D. S., Zhdanova, I. V. and Kishi, S. (2007). Differential effects of genotoxic stress on both concurrent body growth and gradual senescence in the adult zebrafish. *Aging Cell* **6**, 209-224.
van Tuyn, J., Atsma, D. E., Winter, E. M., van der Velde-van Dijke, I., Pijnappels, D. A., Bax, N. A., Knaan-Shanzer, S., Gittenberger-de Groot, A. C., Poelmann, R. E., van der Laarse, A. et al. (2007). Epicardial cells of human adults can undergo an epithelial-to-mesenchymal transition and obtain characteristics of smooth muscle cells in vitro. *Stem Cells* **25**, 271-278.
Warren, K. S., Baker, K. and Fishman, M. C. (2001). The slow mo mutation reduces pacemaker current and heart rate in adult zebrafish. *Am. J. Physiol. Heart Circ. Physiol.* **281**, H1711-H1719.
Yelon, D., Ticho, B., Halpern, M. E., Ruvinsky, I., Ho, R. K., Silver, L. M. and Stainier, D. Y. (2000). The bHLH transcription factor hand2 plays parallel roles in zebrafish heart and pectoral fin development. *Development* **127**, 2573-2582.